communications physics

ARTICLE

Check for updates

https://doi.org/10.1038/s42005-023-01323-9 OPEN

Nonlinear interactions between vibration modes with vastly different eigenfrequencies

Oriel Shoshani [1✉] & Steven W. Shaw [2]

Nonlinear interactions between modes with eigenfrequencies that differ by orders of magnitude are ubiquitous in various fields of physics, ranging from cavity optomechanics to aeroelastic systems. Simplifying their description to a minimal model and grasping the essential physics is typically a system-specific challenge. We show that the complex dynamics of these interactions can be distilled into a single generic form, namely, the Stuart-Landau oscillator. With our model, we study the injection locking and frequency pulling of a low-frequency mode interacting with a blue-detuned high-frequency mode, which generate frequency combs. Such combs are tunable around both the high and low carrier frequencies. By discussing the analogy with a simple mechanical system model, we offer a minimalistic conceptual view of these complex interactions originating the frequency combs, together with showcasing their frequency tunability.

[1] Ben-Gurion University of the Negev, Beer-sheva 84105, Israel. [2] Florida Institute of Technology, Melbourne, FL 32901, USA. ✉email: oriels@bgu.ac.il

Nonlinear interactions of modes with vastly different eigenfrequencies (VDE) are unique because, unlike standard internal resonances[1–5], the eigenfrequencies need not be rationally related. In VDE modes, interactions occur between the envelope of the high-frequency (HF) carrier signal and the oscillations of the low-frequency (LF) carrier signal (Fig. 1). While these VDE modal interactions are peculiar, they are ubiquitous and occur in a wide range of fields of physics. Examples include (i) cavity optomechanics[6–13] and plasmomechanics[14–18], where these interactions are between HF optical modes and the LF mechanical modes; (ii) interactions between HF nano- and LF micro-mechanical modes[19–21]; (iii) certain classes of aeroelastic instabilities, such as stall flutter[22] and transverse galloping[23], where these interactions are between HF vortex modes of the turbulent wake (the so-called Kármán vortex street) and the LF modes of the elastic structure (Fig. 1); and many other systems[24–36]. These interactions have gained significant interest, particularly in cavity optomechanics[37–45], since they offer novel means to generate engineered quantum states[46–49] and practically unlimited bandwidth for enhanced sensing of acceleration[50], mass[51], force[52], vibration[53], chemical quantities[54], and biological quantities[55].

Nonlinear VDE modal interactions have been of interest for decades[56–66]. However, to the best of our knowledge, no theory presents a simple model that captures the essential physics of these interactions and maps them onto a single generic (normal) form. In this paper, we develop such a theory. In particular, we consider the lowest-order (quadratic) nonlinear modal coupling, and show that VDE modal interactions can be mapped onto the normal form of a supercritical Hopf bifurcation described by the Stuart-Landau oscillator[67,68]. Moreover, we present a simple prototypical pendulums system that exhibits VDE modal interactions and offers a simple conceptual view of the generic characteristics of these interactions.

Results and Discussion

Minimalistic model. To derive a minimalistic model for VDE modal interactions, we consider a pair of driven vibration modes that, by the definition of eigenmodes, are linearly uncoupled. We denote their modal coordinates as (q_0, q_1) and their eigenfrequencies as (ω_0, ω_1), where $\omega_0 \ll \omega_1$. The Hamiltonian of the system is given by $H = H_0 + H_1 + H_{\rm int}$, where $H_{0,1} = (p_{0,1}^2 + \omega_{0,1}^2 q_{0,1}^2)/2 - q_{0,1}F_{0,1}\cos(\omega_{F_{0,1}}t)$ are the Hamiltonians of the individual modes, $p_{0,1}$ are the attendant momenta, $F_{0,1}$ and $\omega_{F_{0,1}}$ are the amplitude and frequency of the modal drives, respectively, and $H_{\rm int} = H_{\rm int}(q_0, q_1)$ is the interaction Hamiltonian, which necessarily couples the modes in a nonlinear way.

We restrict the analysis to the lowest order nonlinearity, and write the following single-term interaction Hamiltonian $H_{\rm int} = \alpha q_0 q_1^2$, which is consistent with the interaction Hamiltonian in cavity optomechanics that generates the radiation-pressure force[42]. We note that the inclusion of a term $\beta q_0^2 q_1$ in the Hamiltonian is also possible; however, its contribution is negligible since it does not promote energy exchange during the interactions of interest. Therefore, with the inclusion of linear dissipation terms, we obtain the following dynamical system (Fig. 2)

$$\ddot{q}_0 + 2\Gamma_0\dot{q}_0 + \omega_0^2 q_0 + \alpha q_1^2 = F_0\cos(\omega_{F_0}t), \tag{1}$$

$$\ddot{q}_1 + 2\Gamma_1\dot{q}_1 + \omega_1^2 q_1 + 2\alpha q_0 q_1 = F_1\cos(\omega_{F_1}t). \tag{2}$$

where the $\Gamma_{1,2}$ are the modal decay rates.

Eqs. (1)-(2) are similar to the modal equations (see Supplementary Note 1) of a pair of biased pendulums that are coupled via stiff torsional spring (Fig. 2), and with the nonlinearities truncated at the quadratic order. Note that in the pendulums system, there is an additional term αq_0^2 in the equation of q_0 (see Supplementary Note 1) that has negligible contribution to the leading order approximation. Therefore, we conceptually associate the LF mode with the symmetric mode of the pendulums $q_0 = (\theta_L + \theta_R)/\sqrt{2}$, and the HF mode with the antisymmetric mode of the pendulums $q_1 = (\theta_L - \theta_R)/\sqrt{2}$ (Fig. 2). We note that Eqs. (1)-(2) can be readily generalized to include multiple LF and HF modes, LF mode nonlinearities, and noise (Methods).

For weakly nonlinear modal interactions ($|\alpha q_1^2/\omega_0^2 q_0| \ll 1$, $|\alpha q_0/\omega_1^2| \ll 1$), light damping [$|2\Gamma_0\dot{q}/(\omega_0^2 q_0)| \ll 1$, $|2\Gamma_1\dot{q}_1/(\omega_1^2 q_1)| \ll 1$], and weak external drives [$|F_1/(\omega_1^2 q_1)| \ll 1$, $|F_0/(\omega_0^2 q_0)| \ll 1$] that operate at near-resonance conditions ($|\omega_{F_0} - \omega_0|/\omega_0 \ll 1$, $|\omega_{F_1} - \omega_1|/\omega_1 \ll 1$), we make the following ansatz for the modal dynamics

$$\begin{aligned} q_0(t) &= \bar{q}_0 + A_0(t)e^{i\omega_{F_0}t} + {\rm cc},\ \dot{q}_0(t) = i\omega_0 A_0(t)e^{i\omega_{F_0}t} + {\rm cc}, \\ q_1 &= A_1(t)e^{i\omega_{F_1}t} + {\rm cc},\ \dot{q}_1(t) = i\omega_{F_1}A_1(t)e^{i\omega_{F_1}t} + {\rm cc}. \end{aligned} \tag{3}$$

Here cc denotes the complex-conjugate of the preceding term, $\bar{q}_0 = -\alpha\langle q_1^2\rangle/\omega_0^2$ is a DC deflection that arises from the time-

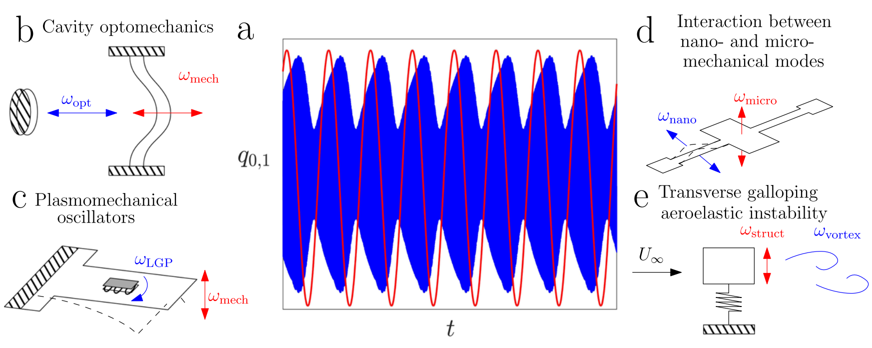

Fig. 1 Nonlinear interactions of modes with vastly different eigenfrequencies (VDE). a The VDE modal interactions are associated with a resonant interaction between the oscillating envelope of the high-frequency mode (blue) and the signal oscillations of the low-frequency mode (red). Examples of systems that exhibit VDE modal interactions include: **b** Cavity optomechanics, where the interaction is between optical (eigenfrequency $\omega_{\rm opt}$) and mechanical (eigenfrequency $\omega_{\rm mech}$) modes. **c** Plasmomechanical oscillators, where the interaction is between localized-gap plasmon (eigenfrequency $\omega_{\rm LGP}$) and mechanical modes (eigenfrequency $\omega_{\rm mech}$). **d** Interactions between nano-mechanical (eigenfrequency $\omega_{\rm nano}$) and micro-mechanical (eigenfrequency $\omega_{\rm micro}$) modes. **e** Aeroelastic instabilities in which the high-speed upstream velocity U_∞ generates a high-frequency turbulent vortex mode in the wake (eigenfrequency $\omega_{\rm vortex}$) that interacts with a low-frequency mode of the mechanical structure (eigenfrequency $\omega_{\rm struct}$).

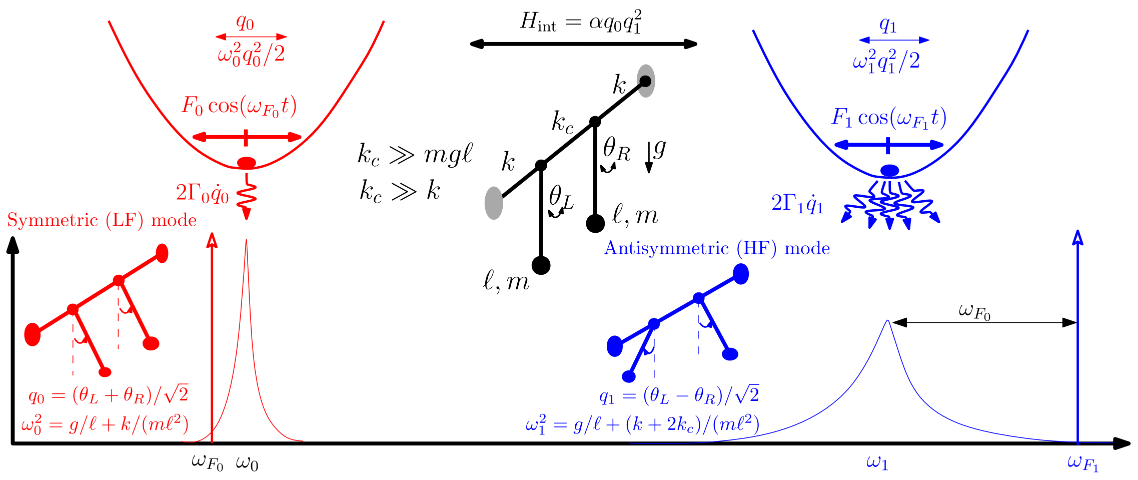

Fig. 2 The minimalistic nonlinear model for interactions between modes with vastly different eigenfrequencies. A pair of linear modes are nonlinearly coupled via the interaction Hamiltonian $H_{\rm int}$. As described in our analysis, we consider the case in which the high-frequency mode (q_1-blue) is driven in its blue sideband with $\omega_{F_1}=\omega_1+\omega_{F_0}$, and its relaxation time is significantly shorter than the relaxation time of the low-frequency mode (q_0-red) $\Gamma_1^{-1}\ll\Gamma_0^{-1}$. The nonlinear pendulums system has similar modal equations and offers a simple conceptual view of these nonlinear modal interactions, where the low-frequency/high-frequency mode corresponds to the symmetric/antisymmetric mode of the pendulums system. The dashed lines of the symmetric/antisymmetric mode represent a nonzero angle, which biases the system and breaks its symmetry. k and k_s are the torsional stiffness of the shafts.

independent component of q_1^2, and $A_{0,1}$ are the complex-amplitudes of the LF and HF modes.

Since $\omega_{F_0}\ll\omega_{F_1}$, we can treat q_0 as a quasi-static variable in Eq. (2) and apply the method of averaging, or equivalently, the rotating wave approximation (RWA) to obtain the following complex-amplitude equations

$$\dot{A}_0=-(\Gamma_0+i\Delta\omega_0)A_0+\frac{i\alpha}{2\pi}\int_t^{t+\frac{2\pi}{\omega_{F_0}}}|A_1|^2 e^{-i\omega_{F_0}t}dt-\frac{iF_0}{4\omega_{F_0}}, \tag{4}$$

$$\dot{A}_1=-\left(\Gamma_1+i\Delta\omega_1\right)A_1+\frac{i\alpha}{\omega_{F_1}}(A_0 e^{i\omega_{F_0}t}+A_0^* e^{-i\omega_{F_0}t})A_1-\frac{iF_1}{4\omega_{F_1}}, \tag{5}$$

where $\Delta\omega_0=\omega_{F_0}-\omega_0$ and $\Delta\omega_1=\omega_{F_1}-\omega_1-\alpha\bar{q}_0/(2\omega_{F_1})$ are the frequency detunings of the LF and HF modes.

A nonstandard feature of Eq (5) is that certain slowly varying excitation effects persist after the RWA, with frequency ω_{F_0}. Specifically, we see that under certain conditions, in particular where A_0 is constant, A_1 can oscillate with a frequency ω_{F_0}. Furthermore, since Eq. (5) is linear in A_1, we can formally solve it in terms of the yet unknown complex amplitude of the LF mode ($A_0=|A_0|e^{i\phi_0}$), i.e., $A_1(t)=e^{-\mathfrak{g}(t)}\{A_{10}-[(iF_1)/(4\omega_{F_1})]\int e^{\mathfrak{g}(t)}dt\}$, where A_{10} is determined from the initial condition of A_1 and $\mathfrak{g}(t)=(\Gamma_1+i\Delta\omega_1)t-i\alpha|A_0|\sin(\omega_{F_0}t+\phi_0)/(\omega_{F_1}\omega_{F_0})$. Consequently, for constant A_0, we can use the Jacobi-Anger expansion to write an explicit formula for the evolution of A_1, e.g., $e^{-i\alpha|A_0|\sin(\omega_{F_0}t+\phi_0)/(\omega_{F_1}\Delta\omega_1)}=\sum_{n=-\infty}^{\infty}J_n(u)e^{-in(\omega_{F_0}t+\phi_0)}$, where $u=\alpha|A_0|/(\omega_{F_1}\omega_{F_0})$, J_n is the $n^{\rm th}$ Bessel function of the first kind, and integrate the resulting expansion term by term. Moreover, since the HF modes typically decay faster than the LF modes, we assume that $\Gamma_1\gg\Gamma_0$, and therefore, q_1 adiabatically tracks q_0 when $t\gg\Gamma_1^{-1}$ (for more details about the adiabatic approximation see[3]). Thus, in the adiabatic tracking regime of q_1, we find that

$$|A_1|^2\equiv f(u)=\left(\frac{F_1}{4\omega_{F_1}}\right)^2 e^{-2\Gamma_1 t}\int e^{[\Gamma_1 t+i(\Delta\omega_1 t-u\sin(\omega_{F_0}t+\phi_0))]}dt\times\int e^{[\Gamma_1 t-i(\Delta\omega_1 t-u\sin(\omega_{F_0}t+\phi_0))]}dt. \tag{6}$$

For $u\leqslant 1$, we use a standard Taylor expansion truncated at cubic order to obtain the approximation $|A_1|^2\approx f(0)+f'(0)u+f''(0)u^2/2+f'''(0)u^3/6$, where $f(0)=[F_1/(4\omega_{F_1}\sqrt{\Gamma_1^2+\Delta\omega_1^2})]^2$ is used to evaluate the DC deflection $\bar{q}_0=-\alpha\langle q_1^2\rangle/\omega_0^2\approx-2\alpha f(0)/\omega_0$ near the onset of VDE modal interactions. By substitution of the truncated expansion of $|A_1|^2$ into Eq. (4), we obtain the following Stuart–Landau oscillator[67,68] for the LF mode

$$\dot{A}_0=(\sigma-l|A_0|^2)A_0-\frac{iF_0}{4\omega_{F_0}}, \tag{7}$$

where

$$\sigma=g_1\frac{\Delta\omega_1}{\omega_{F_1}}\left[2\Gamma_1+i\left(\frac{\Gamma_1^2+\Delta\omega_1^2}{\omega_{F_0}}-\omega_{F_0}\right)\right]-\Gamma_0-i\Delta\omega_0,$$

$$\ell=g_2\frac{\Delta\omega_1}{\omega_{F_1}}\left[\Gamma_1(3\Gamma_1^2+8\omega_{F_0}^2-5\Delta\omega_1^2)+i\left(\frac{\Gamma_1^4-\Delta\omega_1^4}{\omega_{F_0}}+\omega_{F_0}(\Gamma_1^2+5\Delta\omega_1^2-4\omega_{F_0}^2)\right)\right],$$

and $g_{1,2}$ are non-negative quantities given by

$$g_1=\left(\frac{\alpha F_1}{4\omega_{F_1}}\right)^2\prod_{n=-1}^{1}\frac{1}{\Gamma_1^2+(\Delta\omega_1+n\omega_{F_0})^2},$$

$$g_2=\frac{3}{2}\left(\frac{\alpha^2 F_1}{4\omega_{F_1}^2}\right)^2\prod_{n=-2}^{2}\frac{1}{\Gamma_1^2+(\Delta\omega_1+n\omega_{F_0})^2}.$$

Therefore, in the adiabatic regime, the HF mode is functionally dependent on the LF mode. A geometric view of this process is that the faster-decaying dynamics end up on an invariant manifold on which the slower dynamics evolve. The retarded backaction from the HF mode completely modifies the properties of the LF mode. To be specific, we see that at leading order, the interaction between the two modes leads to the following changes in the LF mode: (i) The effective linear damping coefficient $\Gamma_{0eff} \equiv -\Re\{\sigma\} = \Gamma_0 - 2\Gamma_1 g_1 \Delta\omega_1$ can be markedly different from Γ_0. In particular, we find that $\Gamma_{0eff} > \Gamma_0$ for red-detuned drive frequencies (i.e., negative detuning $\Delta\omega_1 < 0$) of the HF mode, and $\Gamma_{0eff} < \Gamma_0$ for blue-detuned drive frequencies (i.e., positive detuning $\Delta\omega_1 > 0$) of the HF mode. Moreover, for sufficiently large HF mode drive amplitude (F_1), Γ_{0eff} becomes negative, and self-induced oscillatory motion, i.e., lasing, is generated in the LF mode. (ii) The linear stiffness effect $\delta\omega_0 A_0 \equiv (\Im\{\sigma\} + \Delta\omega_0)A_0$, shifts the eigenfrequency of the LF mode. For $\delta\omega_0/\omega_0 \ll 1$, the shifted eigenfrequency can be approximated by $\tilde{\omega}_0 \approx \omega_0 + \delta\omega_0$. (iii) The (cubic) nonlinear damping effect $\Re\{\ell\}|A_0|^2 A_0$ introduces a new damping mechanism, which dominates at large amplitudes of the LF mode ($|A_0| \gg \sqrt{|\Re\{\sigma\}/\Re\{\ell\}|}$). And, (iv) the (cubic) nonlinear spring effect $-\Im\{\ell\}|A_0|^2 A_0$ introduces an additional Duffing nonlinearity[69], which yields an amplitude-dependent frequency in the LF mode.

Eq. (7) reveals that the normal form of VDE modal interactions is a simple single-mode nonlinear oscillator, specifically the Stuart–Landau oscillator. Furthermore, Eq. (7) is consistent with the complex-amplitude equation one obtains from the following driven van der Pol–Duffing oscillator[70]

$$\frac{d^2 v}{d\tau^2} - \epsilon(1 - v^2)\frac{dv}{d\tau} + v + \gamma v^3 = F\cos(\Omega_F \tau), \tag{8}$$

where $v = (q_0 - \bar{q}_0)/L$ is the non-dimensional displacement of the LF mode from its equilibrium position ($\bar{q}_0$), and $\tau = t/T$ is the nondimensional time. All other parameters, including characteristic time (T) and length (L) scales, are specified in Supplementary Note 2.

From the foregoing analysis, we deduce that Eq. (8) and Eqs. (1)-(2) are dynamically equivalent when the adiabatic approximation holds. That is, the self-induced oscillations of the LF mode are a manifestation of nonlinear interaction with a blue-detuned HF mode, or alternatively, the leakage of energy from the blue-detuned HF mode generates negative linear damping in the LF mode, which results in self-induced oscillations. While Eq. (8) enables a considerably simpler view of VDE modal interactions, it still possesses an intricate bifurcation structure[71] and can exhibit a wide range of dynamical responses, including chaotic attractors[72]. Consequently, in the remainder of this paper, we focus on a limited range of dynamical responses corresponding to injection locking and pulling of the LF mode. As shown below, injection locking and pulling of the LF mode generate tunable frequency combs in the HF and LF modes, respectively. These tunable frequency combs have potential use in a wide range of applications spanning from frequency metrology[73] to molecular fingerprinting[74].

Frequency combs generation. To explore the injection locking and pulling phenomena of the LF mode, we consider the scenario in which the drive frequency of the HF mode is blue-detuned $\Delta\omega_1 = \omega_{F_0}$ and its amplitude (F_1) is relatively large, such that $\Gamma_{0eff} < 0$ (i.e., self-induced oscillations of the LF mode occur) and $F_0/F_1 \ll 1$ (weak external harmonic injection to the LF mode). Using polar notation for the complex amplitude of the LF mode $A_0 = -\mathrm{i}a_0 \mathrm{e}^{\mathrm{i}[\varphi_0 + \arg(\ell)]}/2$, we find from Eq. (7) that to leading order (Methods), the phase dynamics are governed by the Adler equation[75]

$$\frac{d\varphi_0}{ds} = \Omega_L - \sin\varphi_0, \tag{9}$$

where $s = [F_0|\ell|/(4\omega_{F_0}\sqrt{\Re\{\sigma\}\Re\{\ell\}})]t$ is the non-dimensional time of the Adler equation, and $\Omega_L = 4\omega_{F_0}\Im\{\ell^*\sigma\}\sqrt{\Re\{\sigma\}/\Re\{\ell\}}/(F_0|\ell|)$ is the non-dimensional one-sided frequency-locking range (i.e., the overall locking range of the LF mode is $\pm\Omega_L$ around $\tilde{\omega}_0 t/s$).

Eq. (9) is a reduced-order, simplified, single-dimension dynamical system. To obtain this Adler equation, we effectively eliminate the dynamics of the HF mode (via adiabatic approximation) and then eliminate the amplitude dynamics under the assumption of weak injection (Methods) to achieve an equation for only the phase dynamics. We note that the assumption of weak injection is not mandatory, but it greatly simplifies the analysis. Without this condition, one needs to consider the generalized Adler equation[76], which makes the analysis more complicated, especially when considering the amplitude dynamics.

To integrate Eq. (9), we set $u(s) = \mathrm{e}^{\mathrm{i}\varphi_0(s)}$ and obtain the equation $du/ds = (1 + 2\mathrm{i}\Omega_L u - u^2)/2$, which can be readily solved to yield $u(s) = [(u(0) - u_s)u_{us} - (u(0) - u_{us})u_s \mathrm{e}^{\lambda s}]/[u(0) - u_s - (u(0) - u_{us})\mathrm{e}^{\lambda s}]$, where $u_{s,us} = \mathrm{i}\Omega_L \mp \lambda$ and $\lambda = \sqrt{1 - \Omega_L^2}$. From Eq. (9) and $u(s)$, we see that $|\Omega_L| < 1$ corresponds to injection locking of the LF mode, where for $s \gg \lambda^{-1}$, $\sin\varphi_0 = \Omega_L$, $u = u_s$, and $q_0(t) = \bar{q}_0 + a_0\sin(\omega_{F_0}t + \varphi_0 + \angle\ell)$. The condition $|\Omega_L| < 1$ can be viewed as a case in which the frequency of the external drive in Eq. (8) is close enough to the frequency of the unperturbed limit cycle (i.e., when $F = 0$) such that synchronization/injection-locking is achieved. The injection-locked LF mode, which has constant amplitude and phase, generates a periodically modulated complex-amplitude of the HF mode $A_1(t) = \mathrm{e}^{\mathrm{i}\varphi_1(t)}\sum_n a_{1n}\mathrm{e}^{-\mathrm{i}n(\omega_{F_0}t + \phi_0)}$, where $\varphi_1(t) = \mathrm{i}\alpha a_0\sin(\omega_{F_0}t + \varphi_0 + \angle\ell)/(2\omega_{F_1}\omega_{F_0})$, $a_{1n} = F_1 J_n[\alpha a_0/(2\omega_{F_1}\omega_{F_0})]/[4\omega_{F_1}(\omega_{F_0}(1 - n) - \mathrm{i}\Gamma_1)]$, and J_n is the Bessel function of the first kind. These periodic modulations of A_1 create a frequency comb around ω_1, where the spacing between the spectral lines of the comb is ω_{F_0} (Fig. 3a and b). Therefore, by tuning the injected frequency ω_{F_0}, we can control the spacing of the frequency comb of the HF mode. Injection pulling of the LF mode is associated with $|\Omega_L| > 1$ in which $u(s)$, and therefore, $\varphi_0(s)$ are periodic functions with a period[75] of $2\pi/\sqrt{\Omega_L^2 - 1}$. Alternatively, we can view the condition $|\Omega_L| > 1$ as a case in which the frequency of the external drive in Eq. (8) is not sufficiently close to the frequency of the unperturbed limit cycle such that there are quasi-periodic oscillations of the LF mode. The non-uniform (highly non-harmonic) periodic modulations of φ_0 create a frequency comb around $\tilde{\omega}_0$. The spacing between the spectral lines of the comb is $\sqrt{\Omega_L^2 - 1}(s/t)$ (Fig. 3c and d). Hence, by tuning Ω_L, we can control the spacing of the comb fingers in the spectrum of the LF mode.

Conclusions

We derived and analyzed a simple generic model for the intricate dynamics of VDE modal interactions that occur in a wide class of dynamical systems. We showed that the dynamics of VDE interactions can be mapped onto a single normal form, the Stuart-Landau oscillator, and can be conceptually viewed as the energy exchange between the symmetric and antisymmetric modes of a simple prototypical pendulums system. We studied in detail the phenomena of injection locking and pulling of the LF mode, which corresponds to a blue-detuned HF mode and a weakly driven LF mode. Our study reveales that injection locking and pulling can be exploited to generate tunable frequency combs in both the HF and the LF modes. Furthermore, these frequency combs are outcomes of the phase dynamics of the LF mode, which are governed by the well-known

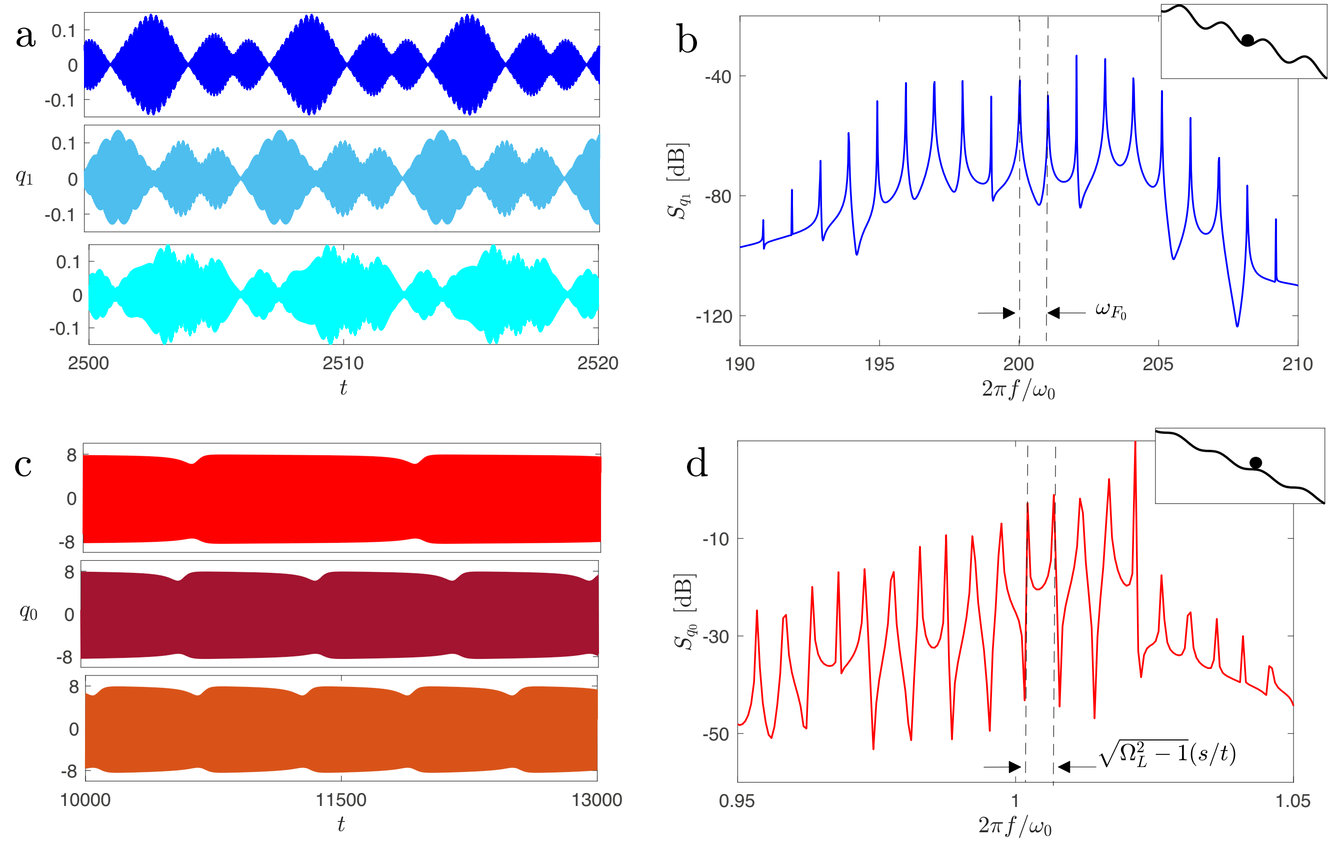

Fig. 3 Injection locking and pulling of the low-frequency mode. a The constant amplitude and phase of the injection-locked low-frequency mode generate periodic modulations in the complex amplitude of the high-frequency mode, **b** which correspond to a frequency comb around ω_1 with a spacing of ω_{F_0} in the power spectral density of q_1. **c** The unlocked phase of the injection-pulled low-frequency mode is periodically modulated in a highly non-uniform rate with a frequency of $\sqrt{\Omega_L^2-1}(s/t)$. Consequently, the temporal responses of the LF mode q_0 are associated with distinct transitions from long calmer epochs to short windows of large modulations, **d** generating a frequency comb around $\tilde{\omega}_0$ with spacing of $\sqrt{\Omega_L^2-1}(s/t)$ in the power spectral density of q_0. All the shown results are obtained from the numerical integration of Eqs. (1)-(2), with $\Gamma_0=0.01, \Gamma_1=0.2$, $\omega_0=1$, $\omega_1=200$, $\alpha=100$, $F_0=0.2$, $F_1=50$, $\omega_{F_1}=\omega_1+\omega_{F_0}$, and ω_{F_0} =0.98 (blue), 1(azure), 1.02 (cyan) in the injection locking regime and ω_{F_0} =1.021(red), 1.022(burgundy), 1.023(orange) in the injection pulling regime.

Adler equation; therefore, injection locking and pulling of the LF mode can be mapped onto the motion of an overdamped particle in a tilted washboard potential (Fig. 3, insets). The study of injection locking and pulling phenomena serves as a showcase for the capabilities of this simple model, which describes generic behavior of these systems and can be used to explore other phenomena, such as cooling and heating of several LF modes (with or without drive), in a straightforward manner.

Methods

A generalized model for VDE modal interactions. To generalize the model of Eqs. (1)-(2), we consider the Hamiltonian $H=H_{\rm lf}+H_{\rm hf}+H_{\rm int}$, where $H_{\rm lf}=\sum_{i=1}^{n}p_{L_i}^2/2+\omega_{L_i}^2q_{L_i}^2/2+\beta_i q_{L_i}^4/4-q_{L_i}F_{L_i}\cos(\omega_{F_{L_i}}t)$ is the Hamiltonian of n low-frequency (LF) modes and each of these modes can have a Duffing nonlinearity (when $\beta_i\neq 0$), $H_{\rm hf}=\sum_{i=1}^{m}p_{H_i}^2/2+\omega_{H_i}^2q_{H_i}^2/2-q_{H_i}F_{H_i}\cos(\omega_{F_{H_i}}t)$ is the Hamiltonian of m high-frequency (HF) modes, and $H_{\rm int}=\sum_{i,j,j'}\alpha_{ijj'}q_{L_i}q_{H_j}q_{H_{j'}}$ is the interaction Hamiltonian and its coefficients $\alpha_{ijj'}$ are symmetric with respect to j and j', i.e., $\alpha_{ijj'}=\alpha_{ij'j}$. With the inclusion of linear dissipation and thermal noise terms (which are connected via the fluctuation-dissipation theorem[77]), we obtain the following dynamical system

$$\ddot{q}_{L_i}+2\Gamma_{L_i}\dot{q}_{L_i}+\omega_{L_i}^2q_{L_i}+\beta_i q_{L_i}^3+\sum_{j,j'}\alpha_{ijj'}q_{H_j}q_{H_{j'}} =F_{L_i}\cos(\omega_{F_{L_i}}t)+\xi_{L_i}(t), \tag{10}$$

$$\ddot{q}_{H_i}+2\Gamma_{H_i}\dot{q}_{H_i}+\omega_{H_i}^2q_{H_i}+2q_{H_i}\sum_j\alpha_{jii}q_{L_j} +2\sum_{j,j'\neq i}\alpha_{jij'}q_{L_j}q_{H_{j'}}=F_{H_i}\cos(\omega_{F_{H_i}}t)+\xi_{H_i}(t), \tag{11}$$

where the Γ_{L_i} and Γ_{H_i} are the modal decay rates, and ξ_{L_i} and ξ_{H_i} are zero-mean delta-correlated independent noise terms, so that $\langle\xi_{L_i}(t)\rangle=\langle\xi_{H_i}(t)\rangle=0$, $\langle\xi_{L_i}(t)\xi_{L_j}(t+\tau)\rangle=2\delta_{ij}\delta(\tau)\mathcal{D}_{\xi_{L_i}}$, and $\langle\xi_{H_i}(t)\xi_{H_j}(t+\tau)\rangle=2\delta_{ij}\delta(\tau)\mathcal{D}_{\xi_{H_i}}$. The above idealization of the noises also applies to general non-Gaussian noises, as long as their correlation times are considerably shorter than the relaxation time of the modes[78].

We make the ansatz

$$\begin{aligned} q_{L_i}(t)&=\bar{q}_{L_i}+A_{L_i}(t)e^{i\omega_{F_{L_i}}t}+\text{cc},\\ \dot{q}_{L_i}(t)&=i\omega_{F_{L_i}}A_{L_i}(t)e^{i\omega_{F_{L_i}}t}+\text{cc},\\ q_{H_i}(t)&=A_{H_i}(t)e^{i\omega_{F_{H_i}}t}+\text{cc},\\ \dot{q}_{H_i}(t)&=i\omega_{F_{H_i}}A_{H_i}(t)e^{i\omega_{F_{H_i}}t}+\text{cc}, \end{aligned} \tag{12}$$

where $\bar{q}_{L_i}=-\langle\sum_{j,j'}\alpha_{ijj'}q_{H_j}q_{H_{j'}}\rangle/\omega_{L_i}^2$ are the DC deflections of the LF modes that arise from the time-independent component of $q_{H_j}q_{H_{j'}}$, and A_{L_i} (A_{H_i}) are the complex-amplitudes of the LF (HF) modes. Treating the q_{L_i} as quasi-static variables in Eq. (11) and applying the rotating wave approximation (RWA), we obtain the following complex-amplitude equations

$$\begin{aligned} \dot{A}_{L_i}=&-\left[\Gamma_{L_i}+i\left(\Delta\omega_{L_i}-\frac{3\beta_i}{2\omega_{F_{L_i}}}|A_{L_i}|^2\right)\right]A_{L_i}\\ &+\frac{i}{2\pi}\sum_{j,j'}\alpha_{ijj'}\int_0^{\frac{2\pi}{\omega_{F_{L_i}}}}A_{H_j}A_{H_{j'}}^{*}e^{i(\omega_{F_{H_j}}-\omega_{F_{H_{j'}}})t}e^{-i\omega_{F_{L_i}}t}dt\\ &-\frac{iF_{L_i}}{4\omega_{F_{L_i}}}-\frac{i}{2\omega_{F_{L_i}}}\langle\xi_{L_i}e^{-i\omega_{F_{L_i}}t}\rangle, \end{aligned} \tag{13}$$

$$\begin{aligned}\dot{A}_{H_i} =& -(\Gamma_{H_i} + \mathrm{i}\Delta\omega_{H_i})A_{H_i} \\ &+ \frac{\mathrm{i}}{2\omega_{F_{H_i}}}\sum_j \alpha_{jii}(A_{L_j}e^{\mathrm{i}\omega_{F_{L_j}}t} + A^*_{L_j}e^{-\mathrm{i}\omega_{F_{L_j}}t})A_{H_i} \\ &+ \frac{\mathrm{i}}{2\pi}\sum_{j,j'\neq i}\alpha_{jij'}A^*_{L_j}A_{H_{j'}}\int_0^{\frac{2\pi}{\omega_{F_{H_i}}}} e^{\mathrm{i}(\omega_{F_{H'_j}} - \omega_{F_{L_j}})t}e^{-\mathrm{i}\omega_{F_{H_i}}t}dt \\ &- \frac{\mathrm{i}F_{H_i}}{4\omega_{F_{H_i}}} - \frac{\mathrm{i}}{2\omega_{F_{H_i}}}\langle\xi_{H_i}e^{-\mathrm{i}\omega_{F_{H_i}}t}\rangle,\end{aligned} \tag{14}$$

where $\Delta\omega_{L_i} = \omega_{F_{L_i}} - \omega_{L_i}$ and $\Delta\omega_{H_i} = \omega_{F_{H_i}} - \omega_{H_i} - \sum_j \alpha_{jii}\bar{q}_{L_j}/(2\omega_{F_{H_i}})$ are the frequency detunings of the LF and HF modes.

Similar to Eq. (5), Eq (14) contains certain slowly varying excitations after the RWA, with frequencies $\omega_{F_{L_i}}$. In particular, for constant A_{L_i}'s, the A_{H_i} oscillate with frequencies $\omega_{F_{L_i}}$. Moreover, from Eq. (14), we see that a pair of HF modes are coupled when they are separated in frequency by one of the LF mode's frequencies, i.e., $|\omega_{H_j} - \omega_{H'_j}| \approx \omega_{L_i}$. Refs. [79,80] show experimental observations of this type of resonant coupling in cavity optomechanical systems. Consequently, Eq. (14) represents a set of linearly coupled equations in A_{H_i}. We can formally solve Eq. (14) in terms of the yet unknown complex amplitudes of the LF modes (A_{L_i}). Then, in the adiabatic tracking regime of A_{H_i} (under the assumption that $\Gamma_{H_i} \gg \Gamma_{L_i}$), we can obtain a set coupled Stuart-Landau oscillators for the complex amplitude of the LF modes. While we leave the details of such an analysis for future study, it is worth noting that even in the case of a single HF mode (and multiple LF modes), its backaction leads to linear and nonlinear coupling between the LF modes. This type of LF modal coupling, which is mediated by the HF modes, has been experimentally observed in Refs. [12,81] in cavity optomechanics. Therefore, Eqs. (13)-(14), which account for the important effects of nonlinearity of the LF modes and noise[8,82], can be viewed as a direct extension of the simplified model of Eqs. (1)-(2), which is clearly relevant to a wider class of systems.

The Adler equation. From Eq. (7), we find that the polar notation $A_0 = -\mathrm{i}a_0 e^{\mathrm{i}[\varphi_0 + \arg(\ell)]}/2$ yields the following pair of equations

$$\dot{a}_0 = \left(\Re\{\sigma\} - \Re\{\ell\}\frac{a_0^2}{4}\right)a_0 - \frac{\varepsilon f_0}{2\omega_{F_0}}\cos\theta, \tag{15}$$

$$\dot{\varphi}_0 = \Im\{\sigma\} - \Im\{\ell\}\frac{a_0^2}{4} - \frac{\varepsilon f_0}{2\omega_{F_0}a_0}\sin\theta, \tag{16}$$

where $\theta = \varphi_0 + \arg(\ell)$, and $\varepsilon f_0 = F_0$, which is used to explicitly denote the smallness of F_0 ($\varepsilon \ll 1$). For $\varepsilon = 0$, the amplitude of the LF mode reaches the steady-state value $a_{0ss} = 2\sqrt{\Re\{\sigma\}/\Re\{\ell\}}$. Thus, in the presence of weak injection, we make the ansatz $a_0(t) = a_{0ss} + \varepsilon\eta(t)$, and obtain the following evolution equation to the perturbation $\dot{\eta} = -2\Re\{\sigma\}\eta - [f_0/(2\omega_{F_0})]\cos\theta$. We see that the perturbation η is strongly damped; hence, for $t \gg 1/\Re\{\sigma\}$, we can set $\dot{\eta} = 0$ to obtain

$$a_0 = 2\sqrt{\frac{\Re\{\sigma\}}{\Re\{\ell\}}} - \frac{\varepsilon f_0}{4\omega_{F_0}\Re\{\sigma\}}\cos\theta. \tag{17}$$

Substitution of Eq. (17) into Eq. (16) yields

$$\begin{aligned}\dot{\varphi}_0 =& \Im\{\sigma\} - \Re\{\sigma\}\frac{\Im\{\ell\}}{\Re\{\ell\}} - \frac{\varepsilon f_0|\ell|}{4\omega_{F_0}\sqrt{\Re\{\sigma\}\Re\{\ell\}}}\sin\varphi_0 \\ &+ O(\varepsilon^2),\end{aligned} \tag{18}$$

which is the well-known Adler equation.

Data availability

The data that support the findings of this study are available from the corresponding author upon reasonable request.

Received: 2 April 2023; Accepted: 26 July 2023;
Published online: 16 August 2023

References

1. Nayfeh, A. H., Lacarbonara, W. & Chin, C.-M. Nonlinear normal modes of buckled beams: three-to-one and one-to-one internal resonances. *Nonlinear Dyn.* **18**, 253–273 (1999).
2. Jeong, B. et al. Utilizing intentional internal resonance to achieve multi-harmonic atomic force microscopy. *Nanotechnology* **27**, 125501 (2016).
3. Shoshani, O. & Shaw, S. W. Resonant modal interactions in micro/nano-mechanical structures. *Nonlinear Dyn.* **104**, 1801–1828 (2021).
4. Li, M. & Haller, G. Nonlinear analysis of forced mechanical systems with internal resonance using spectral submanifolds, part ii: Bifurcation and quasi-periodic response. *Nonlinear Dyn.* **110**, 1045–1080 (2022).
5. Li, M., Jain, S. & Haller, G. Nonlinear analysis of forced mechanical systemswith internal resonance using spectral submanifolds, part i: Periodic response and forced response curve. *Nonlinear Dyn.* **110**, 1005–1043 (2022).
6. Carmon, T., Rokhsari, H., Yang, L., Kippenberg, T. J. & Vahala, K. J. Temporal behavior of radiation-pressure-induced vibrations of an optical microcavity phonon mode. *Phys. Rev. Lett.* **94**, 223902 (2005).
7. Marquardt, F., Harris, J. & Girvin, S. M. Dynamical multistability induced by radiation pressure in high-finesse micromechanical optical cavities. *Phys. Rev. Lett* **96**, 103901 (2006).
8. Bagheri, M., Poot, M., Li, M., Pernice, W. P. & Tang, H. X. Dynamic manipulation of nanomechanical resonators in the high-amplitude regime and non-volatile mechanical memory operation. *Nat. Nanotechnol.* **6**, 726–732 (2011).
9. Favero, I., Sankey, J. & Weig, E. M. Mechanical resonators in the middle of an optical cavity. In *Cavity Optomechanics*, 83–119 (Springer, 2014).
10. Tavernarakis, A. et al. Optomechanics with a hybrid carbon nanotube resonator. *Nat. Commun.* **9**, 1–8 (2018).
11. Sansa, M. et al. Optomechanical mass spectrometry. *Nat. Commun.* **11**, 1–7 (2020).
12. Mercadé, L. et al. Floquet phonon lasing in multimode optomechanical systems. *Phys. Rev. Lett.* **127**, 073601 (2021).
13. Barzanjeh, S. et al. Optomechanics for quantum technologies. *Nat. Phys.* 1–10 (2021).
14. Thijssen, R., Verhagen, E., Kippenberg, T. J. & Polman, A. Plasmon nanomechanical coupling for nanoscale transduction. *Nano Lett.* **13**, 3293–3297 (2013).
15. Zhu, H., Yi, F. & Cubukcu, E. Plasmonic metamaterial absorber for broadband manipulation of mechanical resonances. *Nat. Photo.* **10**, 709–714 (2016).
16. Roxworthy, B. J. & Aksyuk, V. A. Nanomechanical motion transduction with a scalable localized gap plasmon architecture. *Nat. Commun.* **7**, 1–7 (2016).
17. Roxworthy, B. J. & Aksyuk, V. A. Electrically tunable plasmomechanical oscillators for localized modulation, transduction, and amplification. *Optica* **5**, 71–79 (2018).
18. Lee, S. & Seo, M.-K. Full three-dimensional wavelength-scale plasmomechanical resonator. *Optics Lett.* **46**, 1317–1320 (2021).
19. Mahboob, I. et al. Dispersive and dissipative coupling in a micromechanical resonator embedded with a nanomechanical resonator. *Nano Lett.* **15**, 2312–2317 (2015).
20. Sun, F., Dong, X., Zou, J., Dykman, M. I. & Chan, H. B. Correlated anomalous phase diffusion of coupled phononic modes in a sideband-driven resonator. *Nat. Commun.* **7**, 1–8 (2016).
21. Dong, X., Dykman, M. I. & Chan, H. B. Strong negative nonlinear friction from induced two-phonon processes in vibrational systems. *Nat. Commun.* **9**, 1–8 (2018).
22. Dowell, H.*A Modern Course in Aeroelasticity*. Solid Mechanics and Its Applications (Springer International Publishing, 2021).
23. Shoshani, O. Theoretical aspects of transverse galloping. *Nonlinear Dyn.* **94**, 2685–2696 (2018).
24. Naik, A. et al. Cooling a nanomechanical resonator with quantum back-action. *Nature* **443**, 193–196 (2006).
25. Rodrigues, D., Imbers, J. & Armour, A. Quantum dynamics of a resonator driven by a superconducting single-electron transistor: A solid-state analogue of the micromaser. *Phys. Rev. Lett.* **98**, 067204 (2007).
26. Brown, K. R. et al. Passive cooling of a micromechanical oscillator with a resonant electric circuit. *Phys. Rev. Lett.* **99**, 137205 (2007).
27. Murch, K. W., Moore, K. L., Gupta, S. & Stamper-Kurn, D. M. Observation of quantum-measurement backaction with an ultracold atomic gas. *Nat. Phys.* **4**, 561–564 (2008).
28. Vakakis, A. F. et al. *Nonlinear targeted energy transfer in mechanical and structural systems*, vol. 156 (Springer Science & Business Media, 2008).
29. Feng, Z. Instability caused by the coupling between non-resonant shape oscillation modes of a charged conducting drop. *J. Fluid Mech.* **333**, 1–21 (1997).
30. Feng, Z. & Liew, K. Global bifurcations in parametrically excited systems with zero-to-one internal resonance. *Nonlinear Dyn.* **21**, 249–263 (2000).
31. Sheheitli, H. & Rand, R. On the dynamics of a thin elastica. *Int. J. Non-Linear Mech.* **47**, 99–107 (2012).
32. Sheheitli, H. & Rand, R. H. Dynamics of a mass–spring–pendulum system with vastly different frequencies. *Nonlinear Dyn.* **70**, 25–41 (2012).
33. Noël, J.-P., Renson, L. & Kerschen, G. Complex dynamics of a nonlinear aerospace structure: experimental identification and modal interactions. *J. Sound Vibrat.* **333**, 2588–2607 (2014).

34. Claeys, M., Sinou, J., Lambelin, J. & Todeschini, R. Modal interactions due to friction in the nonlinear vibration response of the ?harmony? test structure: Experiments and simulations. *J. Sound Vibrat.* **376**, 131–148 (2016).
35. Roncen, T., Sinou, J.-J. & Lambelin, J.-P. Experiments and simulations of an industrial assembly with different types of nonlinear joints subjected to harmonic vibrations. *J. Sound Vibrat* **458**, 458–478 (2019).
36. Sheheitli, H. & Rand, R. H. Dynamics of three coupled limit cycle oscillators with vastly different frequencies. *Nonlinear Dyn.* **64**, 131–145 (2011).
37. Favero, I. & Karrai, K. Optomechanics of deformable optical cavities. *Nat. Photo.* **3**, 201–205 (2009).
38. Schliesser, A., Arcizet, O., Rivière, R., Anetsberger, G. & Kippenberg, T. J. Resolved-sideband cooling and position measurement of a micromechanical oscillator close to the heisenberg uncertainty limit. *Nat. Phys.* **5**, 509–514 (2009).
39. Anetsberger, G. et al. Near-field cavity optomechanics with nanomechanical oscillators. *Nat. Phys.* **5**, 909–914 (2009).
40. Kippenberg, T. J. & Vahala, K. J. Cavity optomechanics: back-action at the mesoscale. *Science* **321**, 1172–1176 (2008).
41. Purdy, T. P., Yu, P.-L., Peterson, R., Kampel, N. & Regal, C. Strong optomechanical squeezing of light. *Phys. Rev. X* **3**, 031012 (2013).
42. Aspelmeyer, M., Kippenberg, T. J. & Marquardt, F. Cavity optomechanics. *Rev. Modern Phys.* **86**, 1391 (2014).
43. Cattiaux, D. et al. Beyond linear coupling in microwave optomechanics. *Phys. Rev. Res.* **2**, 033480 (2020).
44. Kumar, S. et al. Microwave optomechanical measurement of non-metallized sin strings at mk temperatures. *arXiv preprint arXiv:2110.00228* (2021).
45. Ashour, M., Caspers, J. N., Weig, E. M. & Degenfeld-Schonburg, P. Spontaneous parametric down-conversion induced by optomechanical gradient forces in nanophotonic waveguides. *Phys. Rev. A* **103**, 023513 (2021).
46. Marshall, W., Simon, C., Penrose, R. & Bouwmeester, D. Towards quantum superpositions of a mirror. *Phys. Rev. Lett.* **91**, 130401 (2003).
47. Marquardt, F., Chen, J. P., Clerk, A. A. & Girvin, S. Quantum theory of cavity-assisted sideband cooling of mechanical motion. *Phys. Rev. Lett.* **99**, 093902 (2007).
48. Teufel, J. D. et al. Sideband cooling of micromechanical motion to the quantum ground state. *Nature* **475**, 359–363 (2011).
49. Riedinger, R. et al. Remote quantum entanglement between two micromechanical oscillators. *Nature* **556**, 473–477 (2018).
50. Krause, A. G., Winger, M., Blasius, T. D., Lin, Q. & Painter, O. A high-resolution microchip optomechanical accelerometer. *Nat. Photo.* **6**, 768–772 (2012).
51. Liu, F., Alaie, S., Leseman, Z. C. & Hossein-Zadeh, M. Sub-pg mass sensing and measurement with an optomechanical oscillator. *Opt. Exp.* **21**, 19555–19567 (2013).
52. Allain, P. E. et al. Optomechanical resonating probe for very high frequency sensing of atomic forces. *Nanoscale* **12**, 2939–2945 (2020).
53. Gil-Santos, E. et al. Optomechanical detection of vibration modes of a single bacterium. *Nat. Nanotechnol.* **15**, 469–474 (2020).
54. Venkatasubramanian, A. et al. Nano-optomechanical systems for gas chromatography. *Nano Lett.* **16**, 6975–6981 (2016).
55. Yu, W., Jiang, W. C., Lin, Q. & Lu, T. Cavity optomechanical spring sensing of single molecules. *Nat. Commun.* **7**, 1–9 (2016).
56. Braginski, V. & Manukin, A. Ponderomotive effects of electromagnetic radiation. *Sov. Phys. JETP* **25**, 653–655 (1967).
57. Dykman, M. Heating and cooling of local and quasilocal vibrations by a nonresonance field. *Sov. Phys. Solid State* **20**, 1306–1311 (1978).
58. Haddow, A. & Hasan, S. Nonlinear oscillation of a flexible cantilever: Experimental results. In *Proceedings of the Second Conference on Non-Linear Vibrations, Stability, and Dynamics of Structures and Mechanisms*, 1–3 (1988).
59. Cusumano, J. & Moon, F. Low dimensional behavior in chaotic nonplanar motions of a forced elastic rod: Experiment and theory. In *Nonlinear Dynamics in Engineering Systems*, 59–66 (Springer, 1990).
60. Cusumano, J. P. & Moon, F. Chaotic non-planar vibrations of the thin elastica: Part i: Experimental observation of planar instability. *J. Sound Vibrat.* **179**, 185–208 (1995).
61. Nayfeh, S. & Nayfeh, A. Energy transfer from high- to low-frequency modes in flexible structures. *ASME DES ENG DIV PUBL DE, ASME, NEW YORK, NY(USA), 1992,* **50**, 89–98 (1992).
62. Nayfeh, S. & Nayfeh, A. Nonlinear interactions between two widely spaced modes-external excitation. *Int. J. Bifurcat. Chaos* **3**, 417–427 (1993).
63. Nayfeh, A. H. & Chin, C.-M. Nonlinear interactions in a parametrically excited system with widely spaced frequencies. *Nonlinear Dyn.* **7**, 195–216 (1995).
64. Nayfeh, A. & Mook, D. Energy transfer from high-frequency to low-frequency modes in structures. *J. Vibrat. Acoust.* **117**, 186–195 (1995).
65. Popovic, P., Nayfeh, A. H., Oh, K. & Nayfeh, S. A. An experimental investigation of energy transfer from a high-frequency mode to a low-frequency mode in a flexible structure. *Modal Anal.* **1**, 115–128 (1995).
66. Anderson, T., Nayfeh, A. & Balachandran, B. Coupling between high-frequency modes and a low-frequency mode: Theory and experiment. *Nonlinear Dyn.* **11**, 17–36 (1996).
67. Landau, L. D. On the problem of turbulence. In *Dokl. Akad. Nauk USSR*, vol. 44, 311 (1944).
68. Stuart, J. T. On the non-linear mechanics of hydrodynamic stability. *J. Fluid Mech.* **4**, 1–21 (1958).
69. Lifshitz, R. & Cross, M. C. Nonlinear dynamics of nanomechanical and micromechanical resonators. *Rev. Nonlinear Dyn. Complex.* **1** (2008).
70. Wiggers, V. & Rech, P. C. Multistability and organization of periodicity in a van der pol–duffing oscillator. *Chaos, Solitons Fractals* **103**, 632–637 (2017).
71. Holmes, P. & Rand, D. Bifurcations of the forced van der pol oscillator. *Quart. Appl. Mathe.* **35**, 495–509 (1978).
72. Parlitz, U. & Lauterborn, W. Period-doubling cascades and devil's staircases of the driven van der pol oscillator. *Phys. Rev. A* **36**, 1428 (1987).
73. Udem, T., Holzwarth, R. & Hänsch, T. W. Optical frequency metrology. *Nature* **416**, 233–237 (2002).
74. Thorpe, M. J., Moll, K. D., Jones, R. J., Safdi, B. & Ye, J. Broadband cavity ringdown spectroscopy for sensitive and rapid molecular detection. *Science* **311**, 1595–1599 (2006).
75. Adler, R. A study of locking phenomena in oscillators. *Proc. IRE* **34**, 351–357 (1946).
76. Mirzaei, A., Heidari, M. E., Bagheri, R., Chehrazi, S. & Abidi, A. A. The quadrature lc oscillator: A complete portrait based on injection locking. *IEEE J. Solid-State Circ.* **42**, 1916–1932 (2007).
77. Kubo, R. The fluctuation-dissipation theorem. *Rep. Progress Phys.* **29**, 255 (1966).
78. Stratonovich, R. L.*Topics in the theory of random noise*, vol. 2 (CRC Press, 1967).
79. Kharel, P. et al. High-frequency cavity optomechanics using bulk acoustic phonons. *Sci. Adv* **5**, eaav0582 (2019).
80. Kharel, P. et al. Multimode strong coupling in cavity optomechanics. *Phys. Rev. Appl.* **18**, 024054 (2022).
81. Ren, H. et al. Topological phonon transport in an optomechanical system. *Nat. Commun.* **13**, 1–7 (2022).
82. Leijssen, R., La Gala, G. R., Freisem, L., Muhonen, J. T. & Verhagen, E. Nonlinear cavity optomechanics with nanomechanical thermal fluctuations. *Nat. Commun.* **8**, 1–10 (2017).

Acknowledgements

We wish to thank M.I. Dykman and M.L. Roukes for their critical guidance and invaluable theoretical and experimental insights that contributed significantly to this work. This work is supported by BSF under Grant No. 2018041. SWS is also supported by NSF grant CMMI-1662619. OS is also supported by ISF grant 344/22 and the Pearlstone Center of Aeronautical Engineering Studies at Ben-Gurion University of the Negev.

Author contributions

O.S. and S.W.S. formulated the problem. O.S. developed the analytical approach and conducted the numerical simulations. O.S. and S.W.S. co-wrote the paper.

Competing interests

The authors declare no competing interests.

Additional information

Supplementary information The online version contains supplementary material available at https://doi.org/10.1038/s42005-023-01323-9.

Correspondence and requests for materials should be addressed to Oriel Shoshani.

Peer review information *Communications Physics* thanks Dane D. Quinn and the other, anonymous, reviewer(s) for their contribution to the peer review of this work. A peer review file is available.